Deliverable D11.6:
Report on source specific light absorption characteristics of different anthropogenic and natural aerosol types

Martin Gysel-Beer[1], Rob L. Modini[1], Rosaria E. Pileci[1], Jinfeng Yuan[1], Michele Bertò[1], Nicolas Bukowiecki[1], Athina C. Kalogridis[2], Evangelia Diapouli[2], Kostas Eleftheriadis[2], Angela Marinoni[3], Stefania Gilardoni[3], Birgit Wehner[4], Thomas Müller[4], Thomas Tuch[4], Bas Henzing[5], Marco Zanatta[6], Andreas Herber[6], Eleni Liakakou[7] and Nikos Mihalopoulos[7]

[1]Laboratory of Atmospheric Chemistry, Paul Scherrer Institute, CH-5232 Villigen PSI, Switzerland
[2]N.C.S.R. "DEMOKRITOS", Athens, Greece
[3]Institute of Atmospheric Sciences and Climate, National Research Council of Italy, 40129, Bologna, Italy
[4]Leibniz Institute for Tropospheric Research, Leipzig, Germany
[5]Netherlands Organization for Applied Scientific Research (TNO), Utrecht, the Netherlands
[6]Alfred Wegener Institute (AWI), Helmholtz Centre for Polar and Marine Research, Bremerhaven, Germany
[7]Institute of Environmental Research and Sustainable Development, National Observatory of Athens, 15236, Athens, Greece

Work package no	**WP11 Improving the accuracy of aerosol light absorption determinations**
Deliverable no.	**D11.6**
Lead beneficiary	**PSI / CNRS**
Deliverable type	☑ R (Document, report) ☐ DEC (Websites, patent fillings, videos, etc.) ☐ OTHER: please specify **.....**
Dissemination level	☑ PU (public) ☐ CO (confidential, only for members of the Consortium, incl Commission)
Estimated delivery date	**Month *48***
Actual delivery date	***30/04/2019***
Version	
Comments	

ACTRIS (www.actris.eu) is supported by the European Commission under the Horizon 2020 – Research and Innovation Framework Programme, H2020-INFRAIA-2014-2015, Grant Agreement number: 654109

Motivation, aim and experimental approach

Black carbon (BC) is the main light-absorbing component of atmospheric particulate matter. It is emitted as a by-product of incomplete combustion emissions, namely from combustion engines, wood burning, forest fires or coal burning. The light absorption by BC particles is approximately proportional to the mass of BC, as aerosol particles are similar or smaller than the wavelength of visible solar radiation. Therefore, the aerosol light absorption coefficient ($b_{\mathrm{ap,BC}}$; [Mm^{-1}]) resulting from particulate BC is often inferred from BC mass concentration (m_{BC}; [µg m^3]) using the mass absorption cross-section of BC ($\mathrm{MAC_{BC}}$; [g m^2]):

$$b_{\mathrm{ap,BC}} = \mathrm{MAC_{BC}} \cdot m_{\mathrm{BC}}$$

Therefore, the $\mathrm{MAC_{BC}}$ is a key property remains a key property for e.g. simulating the radiative impacts of atmospheric BC in global simulations in which BC mass concentration is modelled via emissions, atmospheric transport and removal processes. Recently, progress was made using long-term in-situ aerosol observations from the ACTRIS network in better constraining the typical $\mathrm{MAC_{BC}}$ values at European background sites (Figure 1; Zanatta et al., 2016). However, the temporal and spatial variations in $\mathrm{MAC_{BC}}$ are not fully understood. From a theoretical point of view, the $\mathrm{MAC_{BC}}$ does depend on the refractive index of BC (chemical microstructure), the size and the shape of the BC particles, and, most importantly, on the mixing state of BC with other particulate matter. Coatings of organic or inorganic matter internally mixed with BC can increase the $\mathrm{MAC_{BC}}$ of such particles, which is commonly referred to as the "lensing effect". All these particle properties may or may not be systematically related to the BC aerosol source.

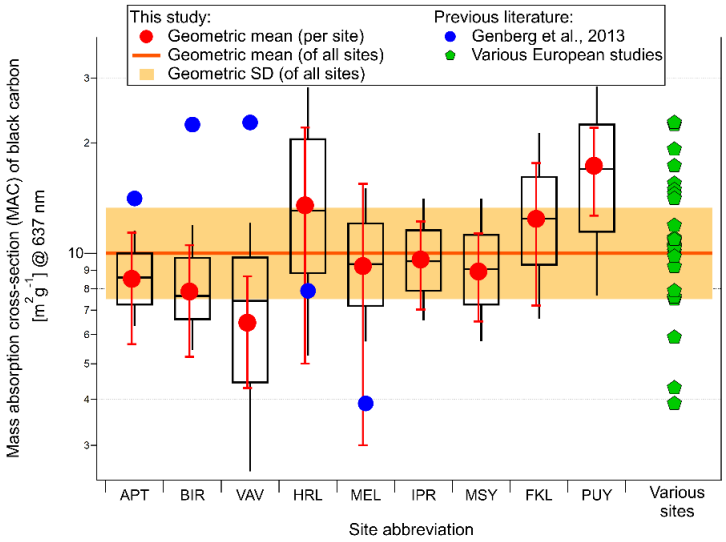

Figure 1 : Mass absorption cross section of BC at European background sites inferred from long-term observations within the ACTRIS network compared with previous literature. (Adapted from Zanatta et al., 2016).

The major sources of BC in Europe are diesel engine exhaust, mainly from traffic, and wood burning emissions, mainly from domestic heating, while other sources such as coal burning may be relevant in certain locations too. Diesel exhaust is dominated by BC with only minor fraction of other co-emitted particulate matter. By contrast, substantial amounts of organic matter is typically co-emitted with BC from wood burning emissions. Some of this organic matter is light absorbing at wavelength shorter than around 500-600 nm, which results in a stronger spectral dependence of the aerosol light absorption coefficient of

ACTRIS (www.actris.eu) is supported by the European Commission under the Horizon 2020 – Research and Innovation Framework Programme, H2020-INFRAIA-2014-2015, Grant Agreement number: 654109

wood combustion aerosol compared to traffic exhaust. It has previously been shown, by comparison against radiocarbon based source apportionment, that this optical feature can be used for BC source apportionment if traffic and wood burning emissions are the only two sources with substantial contributions to total BC (Figure 2; Zotter et al., 2017 and references therein). This approach is commonly referred to as the "aethalometer model". The spectral dependence of the aerosol light absorption with the absorption Ångström exponent (AAE): traffic emissions have an AAE of ~0.9, whereas wood burning emissions have an AAE of ~1.68. The relationship between relative contributions of traffic and wood burning BC and the aerosol AAE according to the aethalometer model is shown in Figure 3.

In this report we assess how the MAC_{BC} depends on BC source and mixing state.

For this purpose, aerosol optical and black carbon properties were measured at multiple ACTRIS sites during dedicated field campaigns. The aethalometer model was chosen for BC source apportionment and a single particle soot photometer was available in some campaigns to quantify the black carbon mixing state with other non-BC particulate matter.

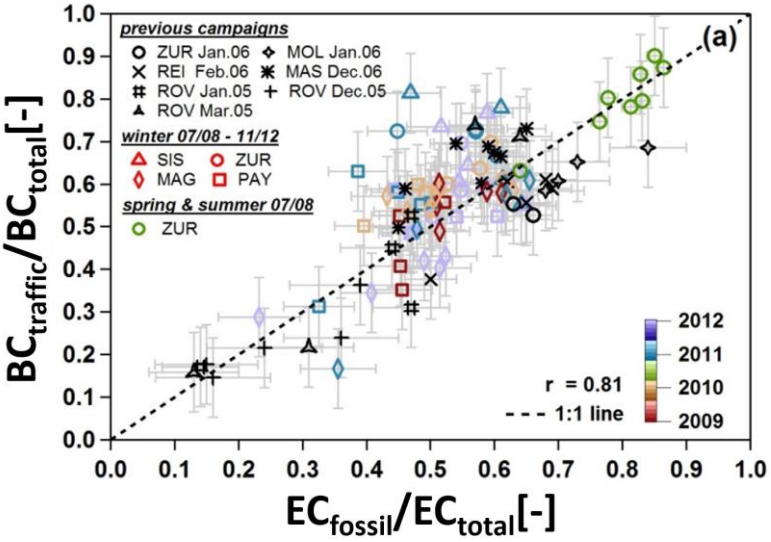

Figure 2: BC source apportionment using the aethalometer model (ordinate) verified against the radiocarbon method (abscissa) for aerosol samples from different locations in Switzerland. Figure taken from Zotter et al. (2017).

ACTRIS (www.actris.eu) is supported by the European Commission under the Horizon 2020 – Research and Innovation Framework Programme, H2020-INFRAIA-2014-2015, Grant Agreement number: 654109

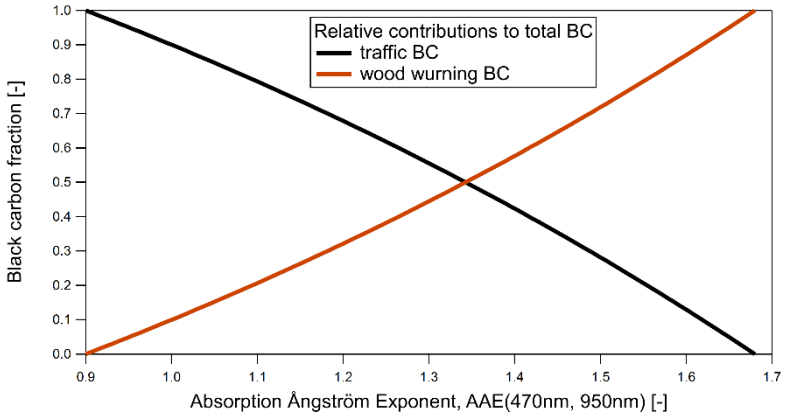

Figure 3: Relative contributions of traffic and wood burning to total BC as a function of aerosol AAE according to the aethalometer model with the model coefficients taken from Zotter et al. (2017) and with assuming that the MAC_{BC} is identical for BC from either source.

Results

Cabauw field experiment

The Cabauw field experiment took place in autumn 2016. Figure 4 shows scatter plots of the observed $\mathrm{MAC_{BC}}$ against BC coating thickness and against AAE. The AAE was usually less than 1.1, indicating that the dominant fraction of BC originated from traffic emissions at any time. More so, BC was largely externally mixed with very little variation in mean coating thickness over time. Lacking substantial variability in aerosol properties and sources in this data set, it is neither possible to make statements on the dependence of $\mathrm{MAC_{BC}}$ on BC mixing state nor on its dependence on BC source.

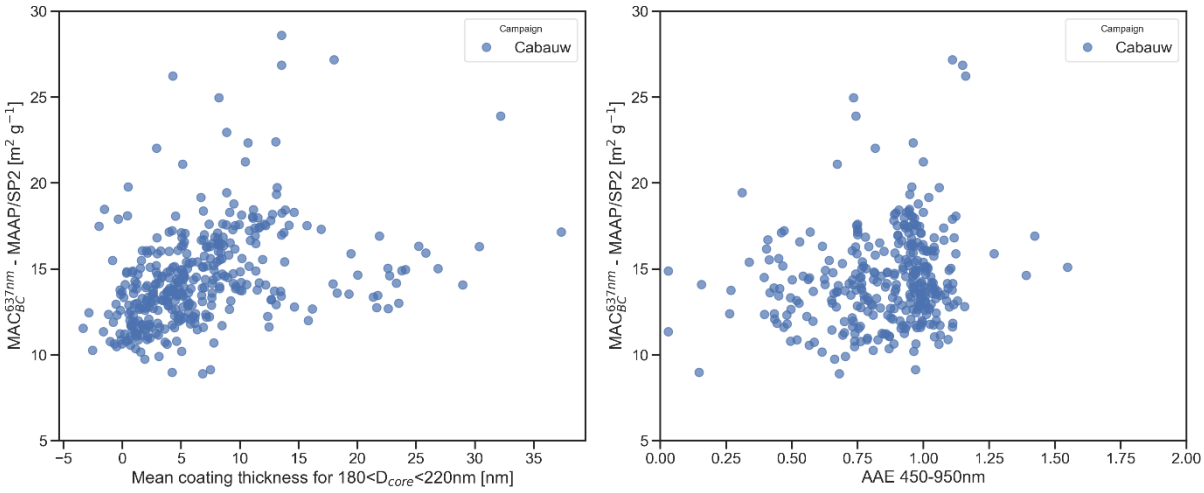

Figure 4: Scatter plots of MAC_{BC} versus BC coating thickness (left panel) and of MAC_{BC} versus AAE as observed during the Cabauw field experiment.

ACTRIS (www.actris.eu) is supported by the European Commission under the Horizon 2020 – Research and Innovation Framework Programme, H2020-INFRAIA-2014-2015, Grant Agreement number: 654109

Melpitz campaign:

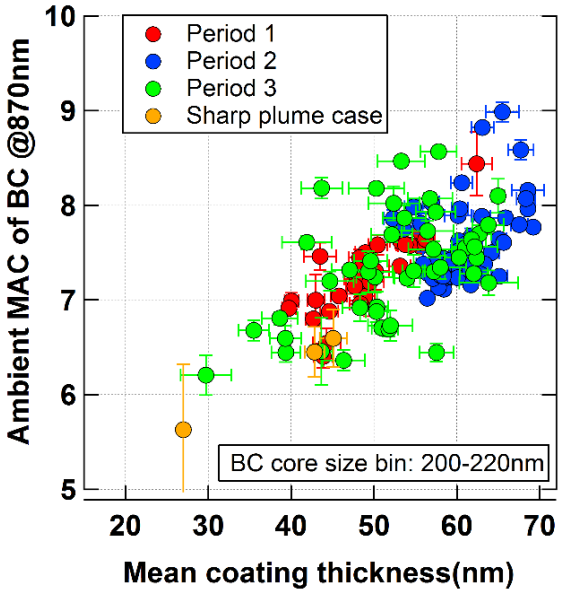

Figure 5: Scatter plot of MAC_{BC} versus BC coating thickness as observed during the Melpitz field experiment. The different colours denote periods with different air mass origin based on back trajectory analyses.

The Melpitz field experiment took place in February 2017. In this experiment, the aerosol properties were more variable than during the Cabauw experiment. Figure 5 shows how the $\mathrm{MAC_{BC}}$ increases with increasing mean BC coating thickness, clearly showing that the lensing effect is the main driver behind variations of the $\mathrm{MAC_{BC}}$. By contrast, no systematic dependence of the $\mathrm{MAC_{BC}}$ on the AAE was observed (Figure 6), indicating that there is no systematic dependence of the $\mathrm{MAC_{BC}}$ on the BC source, also implying that factors other than BC source determine BC coating thickness. Instead, it is likely just the atmospheric age of the BC particles that determines the degree of internal mixing of BC as coatings are acquired through condensation of secondary particulate matter or coagulation of BC with other particles.

ACTRIS (www.actris.eu) is supported by the European Commission under the Horizon 2020 – Research and Innovation Framework Programme, H2020-INFRAIA-2014-2015, Grant Agreement number: 654109

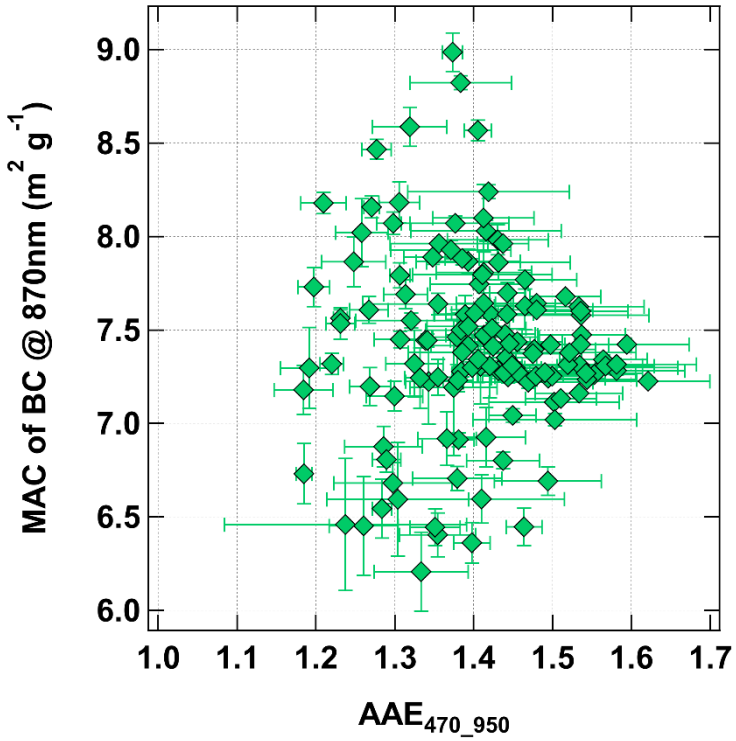

Figure 6: Scatter plot of MAC_{BC} versus AAE as observed during the Melpitz field experiment.

Po Valley campaign:

The Po Valley field experiment took place in summer 2017. The AAE of the aerosol was generally around ~1.2 or less, indicating that during this period the BC was also dominated by traffic sources most of the time (Figure 7), with only very few biomass burning influenced samples. Therefore, it is difficult to make conclusive statements on BC from different sources. However, the BC mixing state exhibited considerable variability as shown in Figure 8 by means of the number fraction of thickly coated BC particles, which is approximately proportional to BC coating thickness. A clear positive correlation between $\mathrm{MAC_{BC}}$ and increasing coating thickness was observed with fresh emissions and aged background air at the extreme ends. This confirms that variations in BC mixing state due to variations in air mass age are the main driver for variations in $\mathrm{MAC_{BC}}$ due to the lensing effect.

ACTRIS (www.actris.eu) is supported by the European Commission under the Horizon 2020 – Research and Innovation Framework Programme, H2020-INFRAIA-2014-2015, Grant Agreement number: 654109

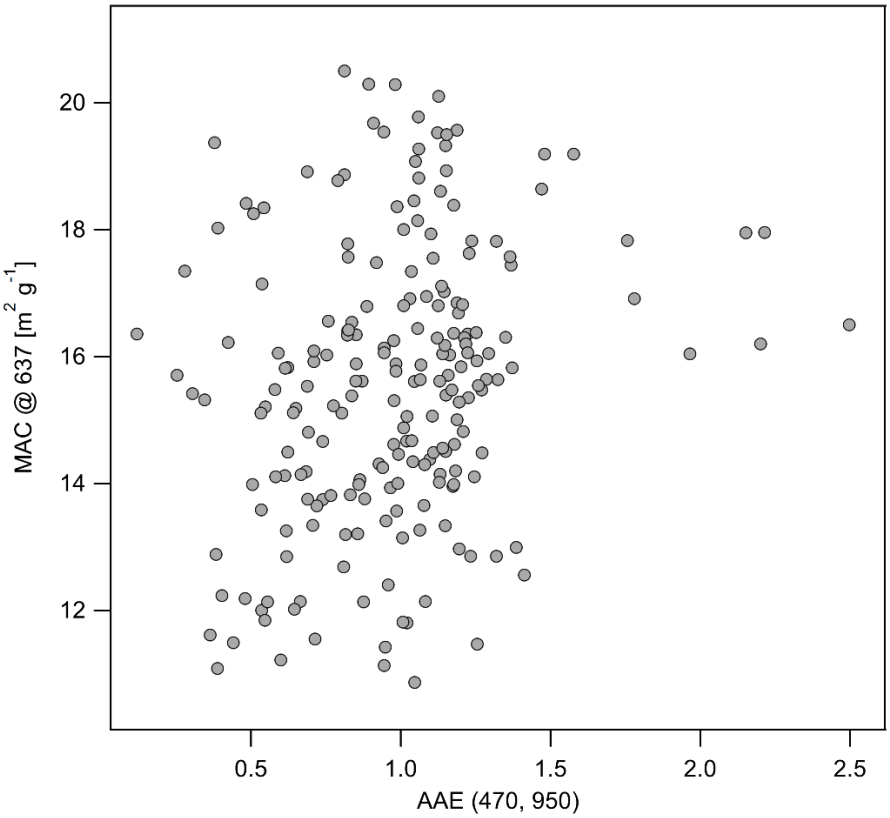

Figure 7: Scatter plot of MAC_{BC} versus AAE as observed during the Po Valley field experiment.

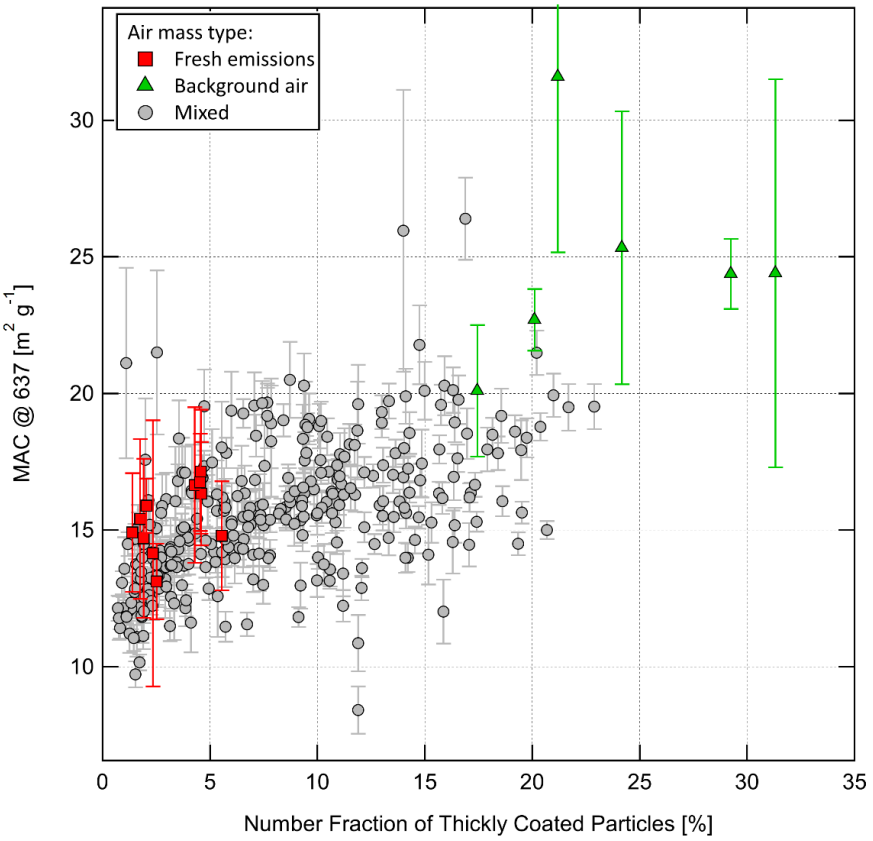

Figure 8: Scatter plot of MAC_{BC} versus number fraction of thickly coated BC particles as observed during the Po Valley field experiment.

ACTRIS (www.actris.eu) is supported by the European Commission under the Horizon 2020 – Research and Innovation Framework Programme, H2020-INFRAIA-2014-2015, Grant Agreement number: 654109

Athens campaign – Demokritos site

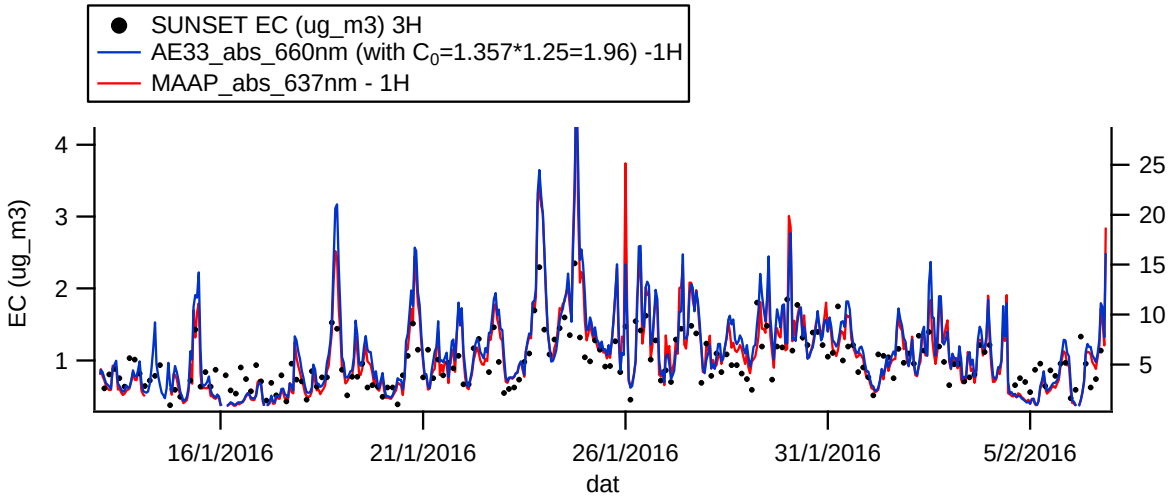

Figure 9: Time series of EC mass concentration (left axis) and aerosol absorption coefficient (right axis) as observed during the Athens field experiment at the Demokritos site.

The Athens field experiment at the suburban Demokritos site took place in January to February 2016. Considerable temporal variations of elemental carbon concentration and aerosol absorption coefficient was observed due to diurnal patterns of emissions and boundary layer dynamics as well as variations in synoptic weather conditions (Figure 9). During wintertime, biomass burning, as inferred from the aethalometer model, contributes between around 20% and 40% of total BC at this suburban site (Figure 10). The observed $\mathrm{MAC_{BC}}$ was independent of the aerosol AAE (Figure 11), i.e. independent of the BC source. More comprehensive results of this experiment in Athens including an additional urban site are published in Kalogridis et al. (2018).

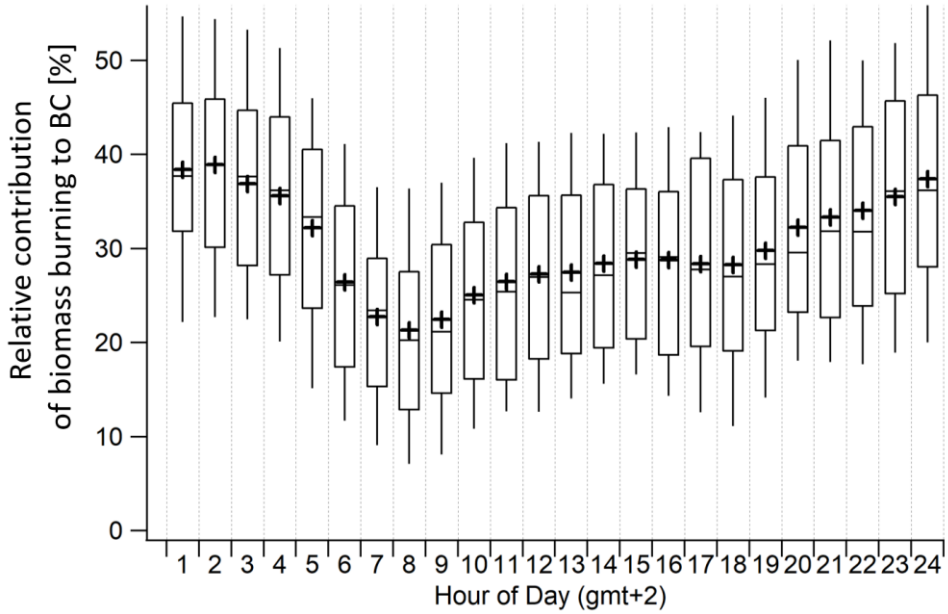

Figure 10: Relative contribution of biomass burning to total BC as observed during the Athens field experiment at the Demokritos site.

ACTRIS (www.actris.eu) is supported by the European Commission under the Horizon 2020 – Research and Innovation Framework Programme, H2020-INFRAIA-2014-2015, Grant Agreement number: 654109

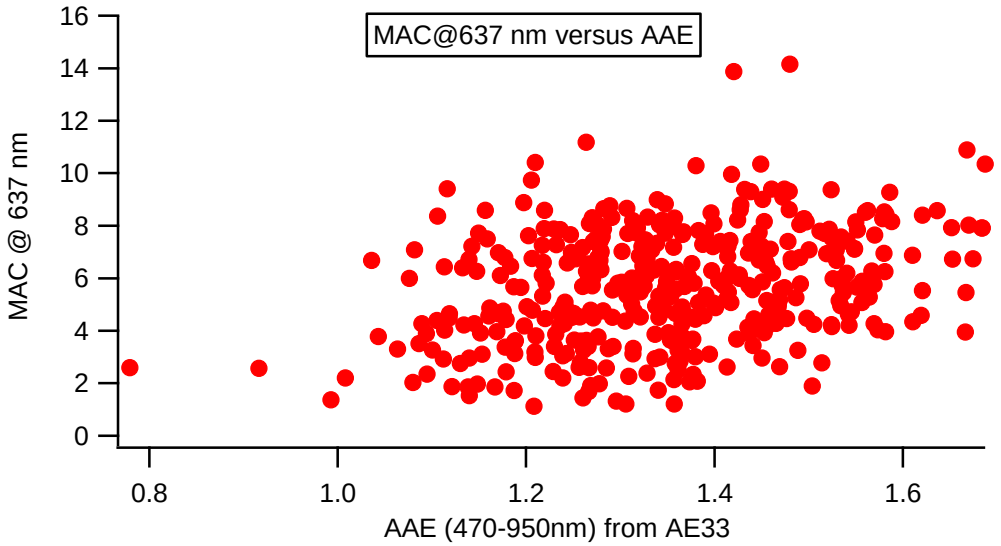

Figure 11: Scatter plot of MAC_{BC} versus AAE as observed during the Athens field experiment at the Demokritos site.

Athens campaign – Thissio site

The field experiment at the urban background site of Thissio situated at the historical centre of Athens during January – February 2016 revealed a pronounced daily and diurnal variability in BC concentration, which maximizes during the morning (8:00-9:00 LST) and evening/night hours (21:00–02:00 LST) respectively (Figure 12). During the campaign period, the morning and evening period-averaged peaks are of similar magnitude (~5-6 μgm^{-3}). Besides variations in local emission rates, meteorology (e.g. rainfall, wind speed, mixing-layer height) strongly controls the daily and diurnal variations of the BC levels. This is also verified by the large variability in the absorption coefficient (Figure 13), which may reach up to 200 Mm^{-1} on certain cases.

The peaks in BC during the morning and evening/night hours are attributed to different sources, which are related to traffic and heating (fossil fuel and wood burning), respectively. This is verified by the diurnal pattern of the relative contribution of wood burning to the BC mass based on the aethalometer model (Figure 14), which reaches a maximum of 30-35% during the night hours, whereas it is minimal (~15%) during the morning rush hour, due to the peak in traffic emissions (fossil-fuel combustion). The correlation between the MAAP absorption coefficient with measured EC from $PM_{2.5}$ samples indicates mean MAC_{BC} of around 7.5 m^2g^{-1} for the field campaign at Thissio site (Figure 15a). No systematic dependence of the MAC_{BC} on the BC source (aerosol AAE) was observed (Figure 15b), which is consistent with the findings at the Demokritos site.

ACTRIS (www.actris.eu) is supported by the European Commission under the Horizon 2020 – Research and Innovation Framework Programme, H2020-INFRAIA-2014-2015, Grant Agreement number: 654109

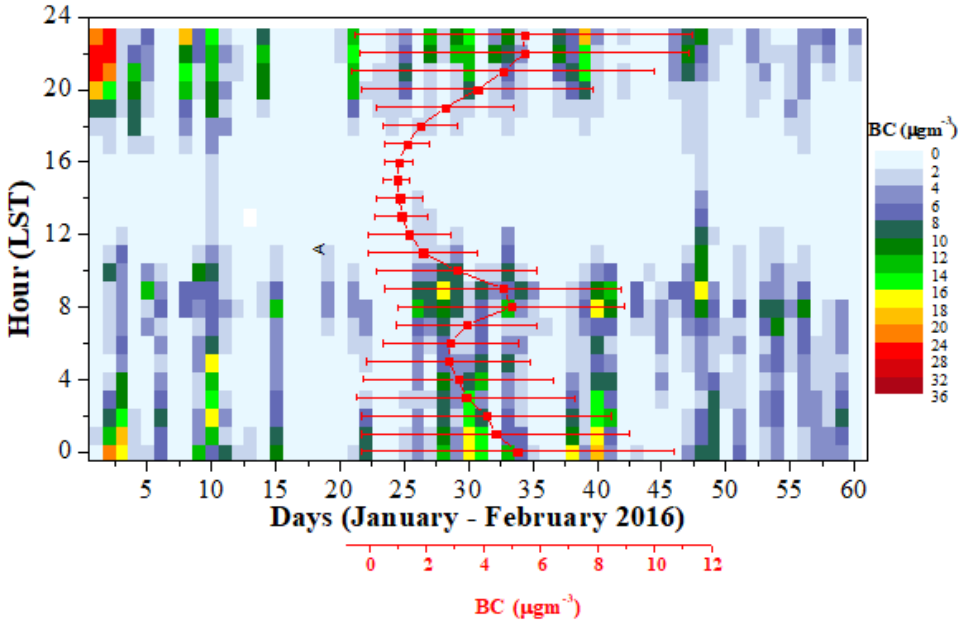

Figure 12: Daily-diurnal contour plot of the BC concentration during the Athens field experiment at Thissio site, superimposed by the period-average diurnal BC pattern.

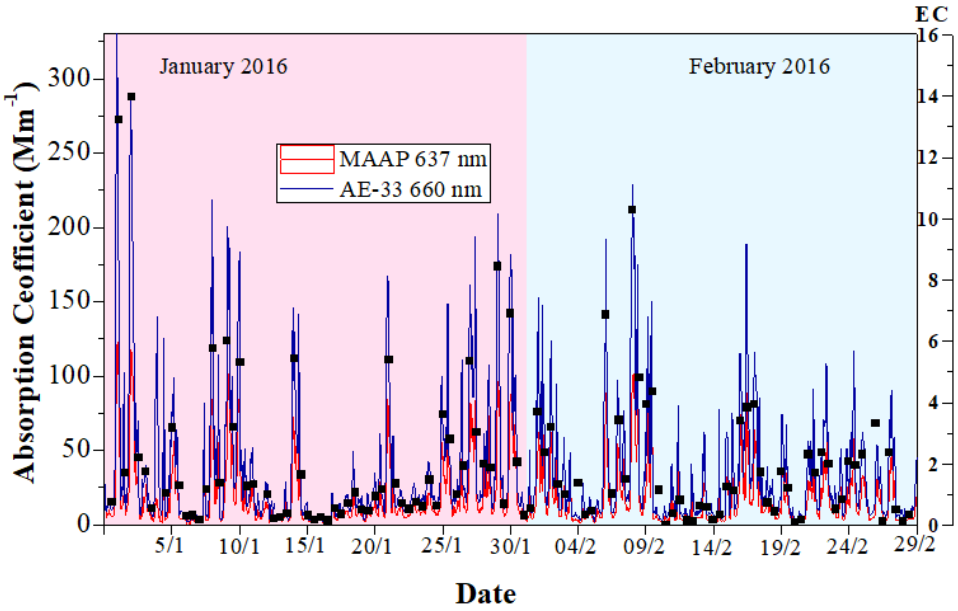

Figure 13: Hourly variation of the absorption coefficient obtained from MAAP at 637nm and from Aethalometer (AE-33) at 660 nm during the Athens experiment at Thissio site. EC on 12hours integrated filters is also depicted (black square values in μg m^{-3}).

ACTRIS (www.actris.eu) is supported by the European Commission under the Horizon 2020 – Research and Innovation Framework Programme, H2020-INFRAIA-2014-2015, Grant Agreement number: 654109

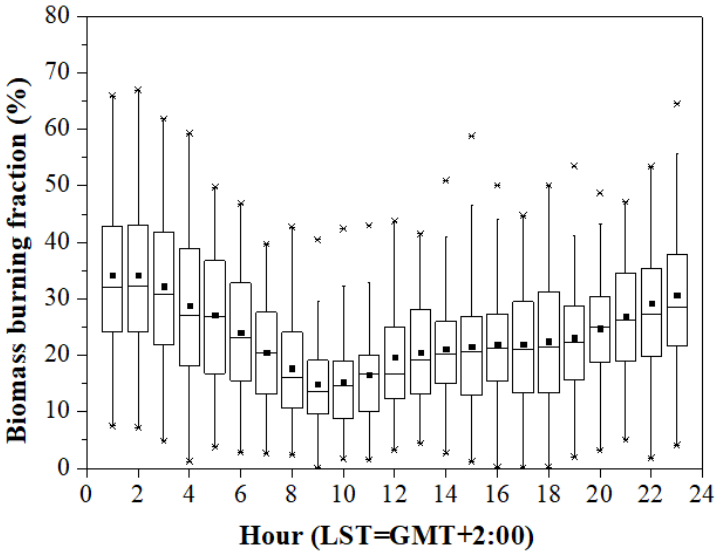

Figure 14: Mean diurnal pattern of the biomass-burning fraction (%) to total BC at Thissio site as inferred using the aethalometer model during January – February 2016.

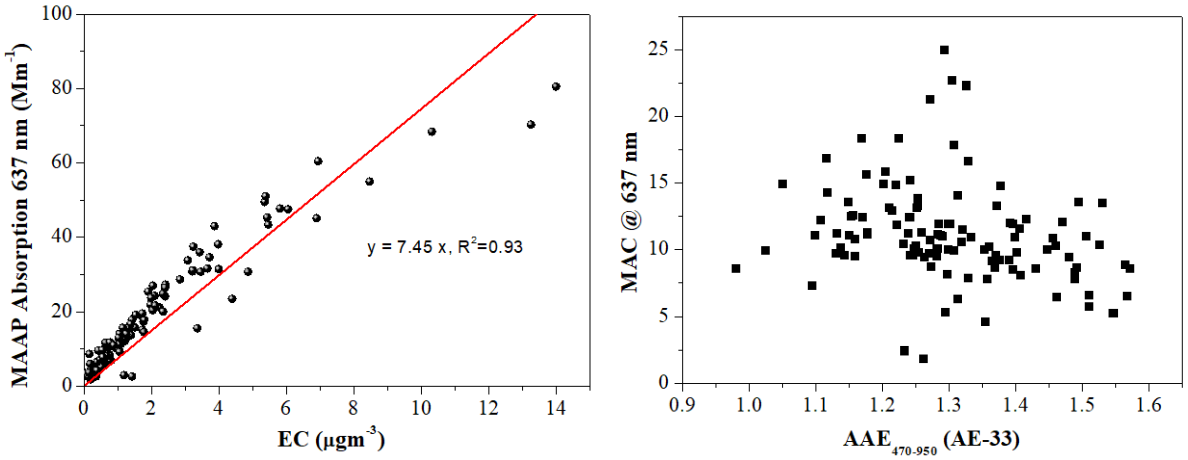

Figure 15: (a) Correlation between MAAP absorption coefficient and EC at Thissio site. The slope of the linear fit through the origin indicates an average MAC_{BC} at 637 nm of around 7.5 m^2/g (b) Time-resolved MAC_{BC} at 637 nm (inferred from MAAP absorption and EC concentrations) versus $AAE_{470-950}$ (inferred from AE-33) at Thissio during January-February 2016.

ACTRIS (www.actris.eu) is supported by the European Commission under the Horizon 2020 – Research and Innovation Framework Programme, H2020-INFRAIA-2014-2015, Grant Agreement number: 654109

Conclusions

- The results do not indicate a significant dependence of $\mathrm{MAC_{BC}}$ on the source of BC.
- Instead, BC mixing state was identified to be the main driver of variations in $\mathrm{MAC_{BC}}$ through the lensing effect, which results in absorption enhancement for internally mixed BC.
- While above-mentioned trends on the source and mixing state dependence are robust, care must be taken with interpreting absolute values of $\mathrm{MAC_{BC}}$ reported here. Different methods were applied to quantify black carbon mass and aerosol absorption coefficient measurements remain tainted with substantial uncertainty, due to a lack of accurate SI traceable methods and transfer standards for either aerosol quantity.

Bibliography

Kalogridis, A. C., Vratolis, S., Liakakou, E., Gerasopoulos, E., Mihalopoulos, N., and Eleftheriadis, K.: Assessment of wood burning versus fossil fuel contribution to wintertime black carbon and carbon monoxide concentrations in Athens, Greece. *Atmos. Chem. Phys.*, **18**, 10219-10236, doi:10.5194/acp-18-10219-2018, 2018.

Zanatta, M., Gysel, M., Bukowiecki, N., Müller, T., Weingartner, E., Areskoug, H., Fiebig, M., Yttri, K. E., Mihalopoulos, N., Kouvarakis, G., Beddows, D., Harrison, R. M., Cavalli, F., Putaud, J. P., Spindler, G., Wiedensohler, A., Alastuey, A., Pandolfi, M., Sellegri, K., Swietlicki, E., Jaffrezo, J. L., Baltensperger, U., and Laj, P.: A European aerosol phenomenology-5: Climatology of black carbon optical properties at 9 regional background sites across Europe. *Atmos. Environ.*, **145**, 346-364, doi:10.1016/j.atmosenv.2016.09.035, 2016.

Zotter, P., Herich, H., Gysel, M., El-Haddad, I., Zhang, Y., Močnik, G., Hüglin, C., Baltensperger, U., Szidat, S., and Prévôt, A. S. H.: Evaluation of the absorption Ångström exponents for traffic and wood burning in the Aethalometer-based source apportionment using radiocarbon measurements of ambient aerosol. *Atmos. Chem. Phys.*, **17**, 4229-4249, doi:10.5194/acp-17-4229-2017, 2017.

ACTRIS (www.actris.eu) is supported by the European Commission under the Horizon 2020 – Research and Innovation Framework Programme, H2020-INFRAIA-2014-2015, Grant Agreement number: 654109